01,11,19

Change in the melting temperature of metals with an increase in pressure

© M.N. Magomedov

Institute for Geothermal Problems and Renewable Energy-branch of Joint Institute for High Temperatures of Russian Academy Sciences,
Makhachkala, Russia

E-mail: mahmag4@mail.ru

Received March 27, 2023
Revised March 27, 2023
Accepted April 7, 2023

A new analytical (i.e., without computer modeling) method for calculating the dependence of the melting temperature T_m of a single-component crystal on pressure P is proposed. The method is based on the delocalization melting criterion and does not contain fitting constants. The baric dependences of the melting temperature $T_m(P)$ and its pressure derivative $T'_m(P)$ for gold, platinum and niobium in the pressure range: $P = 0-1000$ GPa were calculated by this method. It was shown that the dependences calculated by this method for gold and platinum agree better with the experimental data than the dependences obtained by computer simulation methods. For niobium, the calculated dependence $T_m(P)$ turned out to be steeper, i.e., the value $T'_m(P)$ turned out to be larger than in the experiment. It was indicated that this discrepancy might be due both to a decrease in the Lindemann parameter with increasing pressure and to a redistribution of electrons on the s−d-orbitals during compression of transition metals with a BCC structure.

Keywords: melting point, pressure, interatomic interaction, gold, platinum, niobium.

DOI: 10.21883/PSS.2023.05.56040.46

1. Introduction

Dependence of melting temperature T_m on pressure P has bee studied for a long time, however, dependence $T_m(P)$ is still debated even for single-component substances [1–10]. The problem is that the experiments with substance melting at high static pressures and even more so under dynamic have an error which grows with $T-P$ parameters [1–6]. As to theoretical assessments of dependence $T_m(P)$, due to the lack of a theory of the liquid state, there is no theory of melting (or vice versa: due to the lack of a theory of melting, there is no clear idea of single-component liquid). Therefore, it is still not understood why a crystal cannot be overheated above $T_m(P)$, though, a liquid can be overcooled down to $0.8T_m(P)$ easily enough [7].

The main issue with the calculation of substance properties in crystal−liquid phase transition (C−L PT) is the criterium established to determine this transition. Theoretical studies use various phenomenological melting criteria to assess dependence $T_m(P)$ [7,8], and the majority of current studies chose the Lindemann melting criterion [9,10]. The Lindemann melting criterion states that [11,12]: the amplitude of atom vibrations assigned to interatomic distances between the nearest atoms at the melting temperature is constant for crystal with the same structure. The Lindemann criterion was successfully used for theoretical study of melting of single-component crystals with various structures and to calculate the melting parameters of macro- and nanocrystals of various substances [7]. But for a crystallization process, this criterium is not applicable. Therefore, crystallization criteria for a single-component liquid based on diffusion properties of a substance were offered in [13–16].

In [13,14], a Monte Carlo computer-based simulation method was used to investigate argon atom clusters interacting via the Lennard-Jones potential (6−12). It was shown that at the freezing temperature (T_N), the self-diffusion coefficient is constant: $D_f(T_N) \cong 10^{-5}$ cm^2/s, and is independent of the cluster size. Therefore, [13,14] suggested $D_f(T_N) \cong$ const as a crystallization criterion. But since the value of the constant may vary for various substances, this posed a significant limitation for applicability of the criterion. In [15,16] used computer-based molecular dynamics simulation of liquids to offer a „dynamical criterion for freezing“, according to which the following relation is met at the freezing temperature

$$\frac{D_f(T_N)}{D_f(\mathrm{IG})} \cong 0.1,$$

where $D_f(T_N)$ is the self-diffusion coefficient in a liquid phase of the interacting particles at the freezing temperature, $D_f(\mathrm{IG})$ is the Brownian self-diffusion coefficient for the same particles without interaction. It was shown that this crystallization criterion is suitable for various interatomic interaction potentials both for three-dimensional (3D) and two-dimensional (2D)systems. This criterion is applicable to computer-based crystallization simulation of 3D- and 2D-liquids [17], but is not applicable to melting due to uncertainty of function $D_f(\mathrm{IG})$ for a crystal.

In [18,19], we have offered a delocalization criterion for C−L PT according to which C−L PT (in forward and backward direction) starts when the number of delocalized

atoms N_d achieves a certain fraction of the total number of atoms in the system

$$x_d(S \leftrightarrow L) = \frac{N_d(S \leftrightarrow L)}{N} \cong 10^{-2}. \quad (1)$$

Here, $S \leftrightarrow L$ means that this value relates to the solid (S)–liquid (L) transition both in forward and backward directions. It was shown in [18,19] that the delocalization criterion of C–L PT (1) switches to the Lindemann criterion in case of melting, and is reduced to the Löwen criterion in case of crystallization, i.e. it is a generalizing criterion. It was shown in [20,21] that criterion (1) is also applicable to the liquid–glass transition.

A relatively simple analytical (i.e. without computer-based simulation) method for calculation of dependence $T_m(P)$ is offered herein on the basis of criterion (1). The method enables this dependence to be calculated on the basis of only four parameters of the paired Mie–Lennard-Jones interatomic potential, crystal structure, atomic mass and $T_m(0)$ — melting temperature at $P = 0$.

2. Calculation method

To define $x_d(P, T)$, assume a system (crystal or liquid of a single-component substance) consisting of N atoms in the form of a structure composed of $N + N_v$ cells of the same size, where N_v cells are vacant and uniformly distributed over the system volume V. It will be assumed herein that atoms in the system may be in two states: localized and delocalized. In the localized state, an atom is enclosed in a cell formed by the nearest neighbors and has only the vibrational degrees of freedom. In the delocalized state, an atom has access to the whole system volume and has only the translational degrees of freedom. As shown in [19,22], the fraction of delocalized atoms at the given temperature T and specific volume $v = V/N$ of the system is described by the following incomplete gamma-function:

$$x_d(v, T) = \frac{N_d(v, T)}{N} = \frac{2}{\sqrt{\pi}} \int_{E_d/(k_B T)}^{\infty} \sqrt{t} \exp(-t) dt$$

$$= 2 \exp\left(-\frac{E_d}{k_B T}\right) \sqrt{\frac{E_d}{\pi k_B T}} + 1 - \mathrm{erf}\left(\sqrt{\frac{E_d}{k_B T}}\right), \quad (2)$$

where E_d is the energy required for atom transition from the localized to delocalized state, k_B is the Boltzmann constant, and the probability integral is as follows [23]:

$$\mathrm{erf}(x) = \frac{2}{\sqrt{\pi}} \int_0^x \exp(-t^2) dt. \quad (3)$$

Equation (2) is a result of the fact that the number of delocalized atoms having kinetic energy from a certain range of values obeys the Maxwell–Boltzmann distribution which is valid not only to a gas, but also to a liquid, amorphous and crystalline phase [24,25].

Using the Einstein model for the vibrational spectrum of a crystal, the following expression was derived for the atom delocalization energy [18,19,22]:

$$E_d = \left(\frac{3}{8\pi^2}\right) m \left(\frac{3 c_o k_B \Theta_o}{4\hbar \sqrt[3]{k_p}}\right)^2 f_y(y_w). \quad (4)$$

Here, $\hbar$ is Planck's constant, m is the atomic mass, $c_o = [6 k_p V/(\pi N)]^{1/3}$ is the center-to-center distance between the nearest cells in the initial (not relaxed into a vacancy-activated state) vacancy-free (with $N_v = 0$) virtual lattice (indicated by „o"), Θ_o is the Debye temperature for a vacancy-free lattice, k_p is a packing index of a structure composed of $N + N_v$ spherical cells.

The $f_y(y_w)$ function is included in (4) in order to consider quantum effects and is written as

$$f_y(y_w) = \frac{2[1 - \exp(-y_w)]}{y_w[1 + \exp(-y_w)]}, \; y_w = \frac{3\Theta_o}{4T}.$$

From (1)–(4) it follows that the following is satisfied during crystal melting

$$\frac{E_d}{k_B T_m} = \left(\frac{3}{8\pi^2}\right) \frac{k_B m}{T_m} \left(\frac{3 c_o \Theta_o}{4\hbar \sqrt[3]{k_p}}\right)^2 f_y(y_w) \cong 5.672. \quad (5)$$

Expression (5) implies a relation which is functionally in line with the dependence derived by the Lindemann criterion

$$T_m = \left(\frac{3}{8\pi^2}\right) \frac{k_B m}{5.672} \left(\frac{3 c_o \Theta_o}{4\hbar \sqrt[3]{k_p}}\right)^2 f_y(y_w)$$

$$= L_{mE}^2 k_B \frac{m}{3} \left(\frac{3 c_o \Theta_o}{4\hbar}\right)^2 f_y(y_w), \quad (6)$$

where the Lindemann parameter for the vibrational spectrum of the crystal in the Einstein model is defined by the relation [19]:

$$L_{mE} = \frac{3}{\pi \sqrt{8 \cdot 5.672} \cdot \sqrt[3]{k_p}} = \frac{0.142}{\sqrt[3]{k_p}}.$$

Assuming that L_{mE} does not vary with pressure growth, the following expression is easily derived from equation (6)

$$T_m(P) = T_m(0) \left[\frac{c_o(P)\Theta_o(P)}{c_o(0)\Theta_o(0)}\right]^2 \frac{f_y(y_w(P))}{f_y(y_w(0))}. \quad (7)$$

To calculate dependence $c_o(P)\Theta_o(P)$, an equation of state and thermal expansion coefficient of the vacancy-free system shall be known. To define these functions, use the method offered by us in [26].

The pair interatomic interaction will be assumed as the Mie–Lennard-Jones 4-parameter potential written as follows

$$\varphi(r) = \frac{D}{(b-a)}\left[a\left(\frac{r_\mathrm{o}}{r}\right)^b - b\left(\frac{r_\mathrm{o}}{r}\right)^a\right], \quad (8)$$

where D and r_o are the depth and position of the potential minimum, $b > a > 1$ are the parameters.

Then, as shown in [27], within the „only nearest neighbors interaction“ approximation, the Debye temperature may be calculated as

$$\Theta_\mathrm{o}(k_n^\mathrm{o}, c_\mathrm{o}) = A_w(k_n^\mathrm{o}, c_\mathrm{o})\xi\left(-1 + \sqrt{1 + \frac{8D}{k_\mathrm{B}A_w(k_n^\mathrm{o}, c_\mathrm{o})\xi^2}}\right), \quad (9)$$

where k_n^o is the total number of cells (both occupied and vacant) nearest to the atom, $A_w(k_n^\mathrm{o}, c_\mathrm{o})$ arises due to the consideration of „zero vibration“ energy of atoms in the system

$$A_w(k_n^\mathrm{o}, c_\mathrm{o}) = K_\mathrm{R}\frac{5k_n^\mathrm{o}\cdot ab(b+1)}{144(b-a)}\left(\frac{r_\mathrm{o}}{c_\mathrm{o}}\right)^{b+2},$$

$$K_\mathrm{R} = \frac{\hbar^2}{k_\mathrm{B}r_\mathrm{o}^2 m}, \quad \xi = \frac{9}{k_n^\mathrm{o}}. \quad (10)$$

Based on the potential (8), within the „only nearest neighbors interaction“ approximation, the following expression may be derived for the equation of state P and the isothermal modulus of elasticityB_T [26]:

$$P = \left[\frac{k_n^\mathrm{o}}{6}DU'(R) + \frac{9}{4}k_\mathrm{B}\Theta_\mathrm{o}\gamma_\mathrm{o}E_w(y_w)\right]\frac{1}{v}, \quad (11)$$

$$B_T = -v\left(\frac{\partial P}{\partial v}\right)_T = P + \left[\frac{k_n^\mathrm{o}}{18}DU''(R) + \frac{9}{4}k_\mathrm{B}\Theta_\mathrm{o}\gamma_\mathrm{o}(\gamma_\mathrm{o} - q_\mathrm{o})E_w(y_w) - 3k_\mathrm{B}\gamma_\mathrm{o}^2 TF_\mathrm{E}(y_w)\right]\frac{1}{v}. \quad (12)$$

Here, $R = r_\mathrm{o}/c_\mathrm{o} = (v_0/v)^{1/3}$ is the relative linear density of the system,

$$E_w(y_w) = 0.5 + \frac{1}{[\exp(y_w) - 1]},$$

$$F_\mathrm{E}(y_w) = \frac{y_w^2\exp(y_w)}{[\exp(y_w)-1]^2}, \quad v_0 = \frac{\pi r_\mathrm{o}^3}{6k_\mathrm{p}},$$

$$U(R) = \frac{aR^b - bR^a}{b-a},$$

$$U'(R) = R\left[\frac{\partial U(R)}{\partial R}\right] = \frac{ab(R^b - R^a)}{b-a},$$

$$U''(R) = R\left[\frac{\partial U'(R)}{\partial R}\right] = \frac{ab(bR^b - aR^a)}{b-a}. \quad (13)$$

Expressions for the first (γ_o) and second (q_o) Gruneisen parameters for a vacancy-free system that are included in (11) and (12) can be derived from (9). They are written as follows

$$\gamma_\mathrm{o} = -\left(\frac{\partial \ln\Theta_\mathrm{o}}{\partial \ln v}\right)_T = \frac{b+2}{6(1+X_w)},$$

$$q_\mathrm{o} = \left(\frac{\partial \ln\gamma_\mathrm{o}}{\partial \ln v}\right)_T = \gamma_\mathrm{o}\frac{X_w(1+2X_w)}{(1+X_w)}. \quad (14)$$

Here, $X_w = A_w\xi/\Theta_\mathrm{o}$ is introduced, which determines the role of quantum effects in calculating the Gruneisen parameters.

Since, according to (9), the Debye temperature does not depend on temperature during isochoric heating of the system, the isochoric heat capacity and isobaric coefficient of thermal volumetric expansion for the vacancy-free crystal can be calculated as follows [28]:

$$C_v = 3Nk_\mathrm{B}F_\mathrm{E}\left(\frac{3\Theta_\mathrm{o}}{4T}\right),$$

$$\alpha_p = \frac{1}{v}\left(\frac{\partial v}{\partial T}\right)_P = \gamma\frac{C_v}{VB_T} = \frac{\gamma C_v}{NB_T[\pi r_\mathrm{o}^3/(6k_\mathrm{p})]}\left(\frac{v_0}{v}\right). \quad (15)$$

Expressions (8) to (15) define the baric dependence of $c_\mathrm{o}(P)\Theta_\mathrm{o}(P)$ along a certain isotherm. For isotherm $T_\mathrm{m}(0)$, we derive the following expression from (7)

$$T_\mathrm{m}(P, T_\mathrm{m}(0)) = T_\mathrm{m}(0)\left[\frac{c_\mathrm{o}(P, T_\mathrm{m}(0))\Theta_\mathrm{o}(P, T_\mathrm{m}(0))}{c_\mathrm{o}(0, T_\mathrm{m}(0))\Theta_\mathrm{o}(0, T_\mathrm{m}(0))}\right]^2 \times \frac{f_y(y_w(P, T_\mathrm{m}(0)))}{f_y(y_w(0, T_\mathrm{m}(0)))}. \quad (16)$$

With isothermal pressure growth, $c_\mathrm{o}(P, T_\mathrm{m}(0))$ decreases, but $T_\mathrm{m}(P, T_\mathrm{m}(0))$ from (16) grows. Growth of $T_\mathrm{m}(P, T_\mathrm{m}(0))$ should result in the corresponding increase in $c_\mathrm{o}(P, T_\mathrm{m}(0))$. To consider this effect, the contribution made by the functions included in (16) shall be addressed. At high temperatures (i.e. at $T \gg \Theta_\mathrm{o}$), $f_y(y_w)$ is close to unity: $f_y(y_w \ll 1) \cong 1$. Therefore, the ratio of these functions in (16) may be assumed equal to 1. Under the condition (that is satisfied for all metals)

$$\frac{8D}{k_\mathrm{B}A_w(k_n^\mathrm{o}, c_\mathrm{o})\xi^2} \gg 1,$$

equation (9) may be simplified to:

$$\Theta_\mathrm{o}(k_n^\mathrm{o}, c_\mathrm{o}) \cong \left[\frac{8DA_w(k_n^\mathrm{o}, c_\mathrm{o})}{k_\mathrm{B}}\right]^{1/2} = \left[\frac{5\hbar^2 Dk_n^\mathrm{o}ab(b+1)}{18k_\mathrm{B}^2 mr_\mathrm{o}^2(b-a)}\left(\frac{r_\mathrm{o}}{c_\mathrm{o}}\right)^{b+2}\right]^{1/2}.$$

Hence, the following relation can be easily derived

$$[c_\mathrm{o}(P)\Theta_\mathrm{o}(P)]^2 \cong \frac{5\hbar^2 Dk_n^\mathrm{o}\cdot ab(b+1)}{18k_\mathrm{B}^2 m(b-a)}\left(\frac{r_\mathrm{o}}{c_\mathrm{o}(P)}\right)^b.$$

Thus, the contribution of the increase in $c_o(P, T_m(0))$ with baric growth of the melting temperature from $T_m(0)$ to $T_m(P, T_m(0))$ may be considered by introduction of additional term into (16)

$$T_m(P) \cong T_m(P, T_m(0)) \times \exp\left[-\frac{b}{3}\alpha_p(P, T_m(0))\left[T_m(P, T_m(0)) - T_m(0)\right]\right], \quad (17)$$

where $\alpha_p(P, T_m(0))$ is the thermal expansion coefficient at pressure P calculated using equation (15) along isotherm $T_m(0)$.

3. Calculation results

3.1. Gold

Gold (Au, $m(\mathrm{Au}) = 196.967$ a.m.u.) at $P = 0$ has a melting temperature equal to $T_m(0) = 1337$ K [5]. Gold has a face-centered cubic (FCC) structure ($k_n^o = 12$, $k_p = 0.7405$) and does not experience polymorphic phase transitions up to 220 GPa [29]. Therefore, FCC-Au is used as a pressure standard [30].

The parameters of pair interatomic potential for FCC-Au (8) were determined by us using a self-consistency method in [31], and have the following values:

$$r_o = 2.87 \cdot 10^{-10}\,\mathrm{m}, \quad D/k_B = 7446.04\,\mathrm{K},$$

$$b = 15.75, \quad a = 2.79. \quad (18)$$

The equation of state and FCC-Au parameters with interatomic potential parameters (18) were calculated by the method from (8)–(15) in [26]. The results obtained in [26] showed good agreement with the experimental data. Therefore, to calculate $T_m(P)$, we used (18). When using potential parameters (18), the following expressions were derived using equations (9)–(15) along isotherm $T_m(0) = 1337$ K at $P = 0$ for the parameters included in equation (16):

$$c_o(0, T_m(0)) = 2.93432 \cdot 10^{-10}\,\mathrm{m},$$

$$\Theta_o(0, T_m(0)) = 168.28\,\mathrm{K}.$$

Figure 1 shows baric dependences both for the melting temperature $T_m(P)$ (left graphs) and for the melting temperature derivative with respect to pressure: $T_m'(P) = dT_m/dP$ (right graphs) for FCC-Au. Functions $T_m'(P)$ were calculated by means of numerical differentiation of isothermal dependences from (16) and (17) with respect to pressure. The upper graphs show the low pressure region 0–20 GPa; the central graphs show 0–150 GPa region; the lower graphs show 0–1000 GPa region. Dotted lines show dependences $T_m(P)$ and $T_m'(P)$ calculated by us using equations (16) (upper line) and (17) (lower line). Experimental data for $T_m(P)$ are shown by the following symbols: crosses — from [2] and circles — from [5]. Solid lines — are the dependences obtained in [4] and [5] by fitting the experimental data to the Simon–Glatzel equation written as:

$$T_m(P) = T_{m0}\left[1 + \frac{P}{P_0}\right]^{c_s}, \quad (19)$$

$$T_m'(P) = \frac{dT_m(P)}{dP} = T_{m0}\frac{c_s}{P_0}\left[1 + \frac{P}{P_0}\right]^{c_s - 1}. \quad (20)$$

In [4] for FCC-Au for the pressure region up to 6 GPa, $T_{m0} = 1339$ K, $P_0 = 16.1$ GPa, $c_s = 0.57$. were obtained In [5] for FCC-Au for the region up to 106 GPa, $T_{m0} = 1337$ K, $P_0 = 22.265 \pm 1.83$ GPa, $c_s = 0.662 \pm 0.03$ were obtained.

Also, in [5], dependence $T_m(P)$ was calculated by the molecular dynamics method. For this dependence at pressures up to 107 GPa, $T_{m0} = 1181$ K, $P_0 = 17.94$ GPa, $c_s = 0.709$ were obtained. This calculated dependence is shown by a dashed line in Figure 1.

As shown in Figure 1 and Table 1 for FCC-Au, our dependence (17) is in line with the experimental dependences from [4,5] better than the dependence obtained in [5] by the molecular dynamics method up 200 GPa. But it should be considered that dependence (19) was obtained in [4] for the pressure region up to 6 GPa, and in [5] — for the region up to 106 GPa.

It should be noted that dependence $T_m(P)$ for FCC-Au was also calculated by various analytical methods in [9,32–34], where good agreement with the experimental data was achieved (see Table 1). However, in [9,32] for transformation of volumetric dependences into baric dependences, various phenomenological equations were used. In [9], the Stacey equation of state was used. In [32], for this purpose, the Vinet equation of state and relation $\gamma = \gamma_0(V/V_0)^q$, where $q = 1$ was postulated for the second Gruneisen parameter. In [33,34], calculations were carried out using the statistical moments method, SMM. SMM from [33,34] is also based on the Mie–Lennard-Jones pair interatomic interaction potential (8). However, SMM is

Table 1. Experimental and theoretical (in brackets) values of the melting line inclination at $P = 1$ bar for FCC-Au

Authors — year	dT_m/dP, K/GPa	Ref.
Mitra *et al.* — 1967	59.7 ± 3 (60–66)	[1]
Akella & Kennedy — 1971	57.3 (60–66)	[2]
Mirwald & Kennedy — 1979	57.0	[3]
Errandonea — 2010	47 ± 3 (37)	[4]
Hieu & Ha — 2013	(38.18–42.66)	[32]
Weck *et al.* — 2020	39.55* (46.6)*	[5]
Ashwini *et al.* — 2022	(43.32)	[9]
Van Nghia *et al.* — 2022	(40.4)	[34]
This work:		
Eq. (16)	(63.410)	
Eq. (17)	(35.824)	

Comment. * Defined using equation (20) with parameters from the referenced paper.

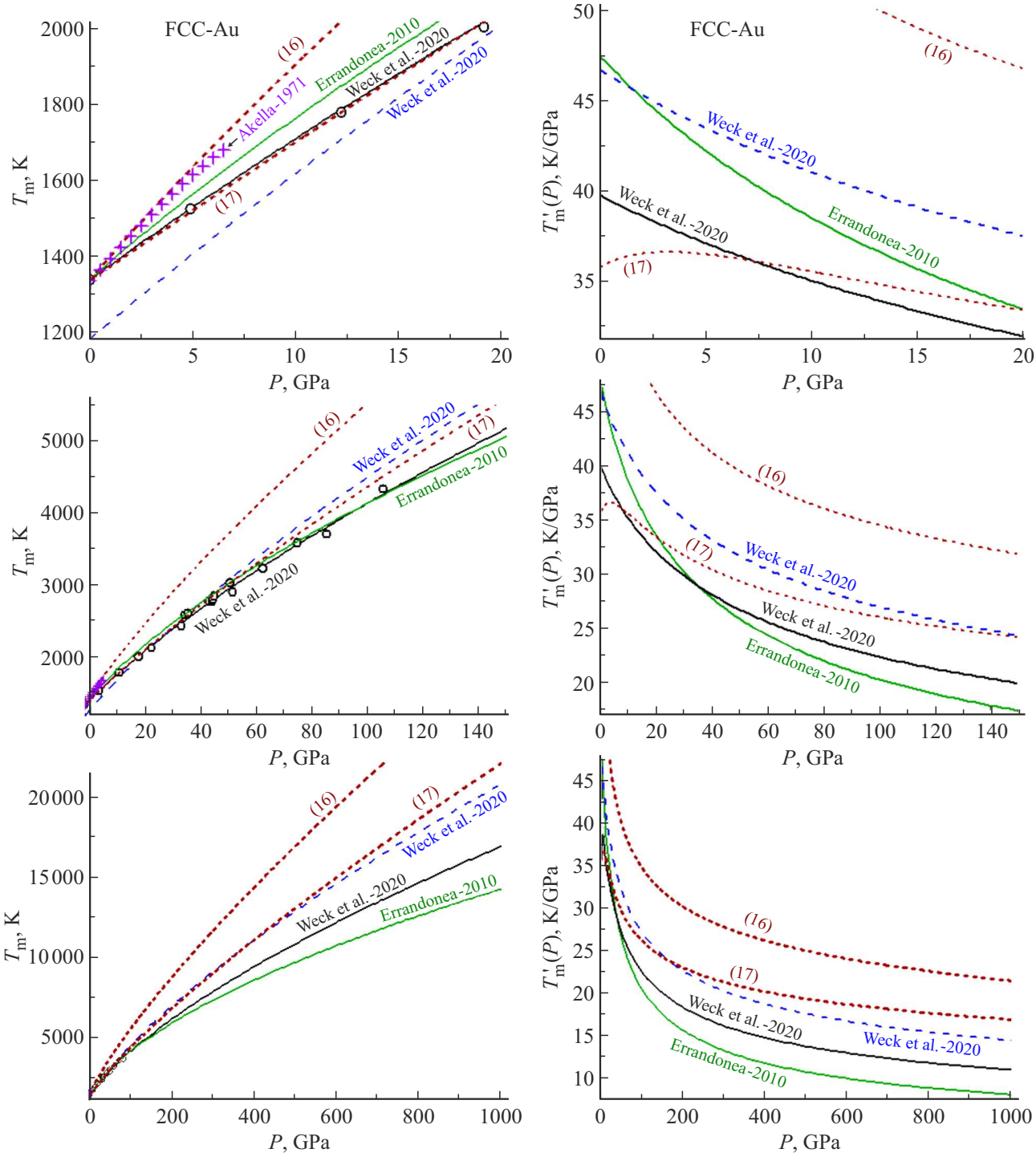

Figure 1. Baric dependences of melting temperature $T_m(P)$ (left graphs) and functions $T'_m(P)$ (right graphs) for FCC-Au. Experimental data for $T_m(P)$ are shown by the following symbols: crosses — from [2], circles — from [5]. Solid lines — dependences (19) and (20) obtained in [4,5] on the basis of the experimental data. Dashed lines — calculated dependences (19) and (20) obtained in [5]. Dotted lines — our calculations using equations (16) — upper line, and (17) — lower line.

much more sophisticated that our method from (8)–(17). Moreover, we use the potential parameters (8), that were defined using a self-consistency method from (8)–(15) in [31]. For calculations within SMM, potential parameters (8) were taken from other studies, where these parameters were defined by other methods. In [33], for transformation of volumetric dependences to baric dependences, power approximation of the equation of state of gold obtained at $T = 0$ K was used. In [34], dependences $P(V, T)$ for Au were not presented. Therefore, the issue

of correct pressure calculation by the method used in [34] remains open.

3.2. Platinum

Baric dependence $T_m(P)$ for platinum was experimentally studied in [1,35–38]. Platinum (Pt, $m(\mathrm{Pt}) = 195.08$ a.m.u.) has a FCC structure ($k_n^o = 12$, $k_p = 0.7405$) and does not experience polymorphic phase transitions up to 200 GPa [37,38]. Therefore, platinum, along with gold, is used as a pressure standard [30]. However, the experimental data from [1,35–38] for dependence $T_m(P)$ is very inconsistent which is caused by the refractory property of this metal [39]. At $P = 0$ the melting point of platinum is equal to $T_m(0) = 2041.7$ K [37].

Pair interatomic potential parameters (8) for FCC-Pt were calculated by the self-consistency method in [31] according to the calculations using the equation of state, thermal expansion coefficient, modulus of elasticity and other properties. They are as follows:

$$r_o = 2.766 \cdot 10^{-10}\,\mathrm{m}, \quad D/k_B = 11400.7\,\mathrm{K},$$

$$b = 11.65, \quad a = 3.05. \tag{21}$$

When using potential parameters (21), the following expressions were derived using equations (9)–(15) along isotherm $T_m(0) = 2041.7$ K at $P = 0$ for the parameters included in equation (16):

$$c_o(0, T_m(0)) = 2.82146 \cdot 10^{-10}\,\mathrm{m},$$

$$\Theta_o(0, T_m(0)) = 221.477\,\mathrm{K}.$$

Figure 2 shows baric dependences both for the melting temperature $T_m(P)$ (left graphs) and for the melting temperature derivative with respect to pressure: $T_m'(P) = dT_m/dP$ (right graphs) for FCC-Pt. The upper graphs show the low pressure region 0–20 GPa; the central graphs show 0–150 GPa region; the lower graphs show 0–1000 GPa pressure region. Dotted lines show dependences $T_m(P)$ and $T_m'(P)$ calculated by us using equations (16) (upper line) and (17) (lower line). Solid circles show experimental data for $T_m(P)$ from [38]. Solid lines — are the dependences obtained in [35,36,38] by fitting the experimental data to the Simon–Glatzel equation (19) with parameters

$T_{m0} = 2042$ K, $P_0 = 21.5$ GPa, $c_s = 0.50$ from [35],
$T_{m0} = 2046$ K, $P_0 = 23.0$ GPa, $c_s = 0.28$ from [36],
$T_{m0} = 2041$ K, $P_0 = 15.1$ GPa, $c_s = 1/2.6 = 0.3846$ from [38].

Dashed lines in Figure 2 show the dependences (19) and (20) found in [37] by ab initio calculations using Z-method and approximated by dependence (19) with parameters

$$T_{m0} = 2041.7\,\mathrm{K}, \; P_0 = 44.0\,\mathrm{GPa}, \; c_s = 0.85.$$

As shown in Figure 2 and Table 2 for FCC-Pt, our dependence (17) agrees with the experimental points from [38] better than the dependence calculated in [37] using Z-method. But it should be considered that dependence parameters (19) were obtained in [35] for the pressure region up to 30 GPa, and in [38] — for the region up to 107 GPa.

Table 2. Experimental and theoretical (in brackets) values of the melting line inclination at $P = 1$ bar for FCC-Pt

Authors — year	dT_m/dP, K/GPa	Ref.
Mitra *et al.* — 1967	42 ± 7	[1]
Errandonea — 2013	47	[35]
Patel & Sunder — 2018	25	[36]
Anzellini *et al.* — 2019	(39.4)*	[37]
Geballe *et al.* — 2021	~ 40 (52)*	[38]
This work:		
Eq. (16)	(45.441)	
Eq. (17)	(33.185)	

Comment. * Defined using equation (20) with parameters from the referenced paper.

3.3. Niobium

Niobium is more refractory material than platinum: $T_m(0) = 2750$ K [40]. Therefore, experimental dependence $T_m(P)$ for niobium has been measured only recently in [40]. Niobium (Nb, $m(\mathrm{Nb}) = 92.9064$ a.m.u.) has a body-centered cubic (BCC) structure ($k_n^o = 8$, $k_p = 0.6802$), though, it is reported that BCC-Nb at $P > 6$ GPa can transfer to orthorhombic Pnma-phase [40]. Dependence $T_m(P)$ for BCC-Nb was theoretically calculated in [40–44] by various methods.

BCC-Nb parameters of pair interatomic potential (8) were determined using a self-consistency method in [42], and have the following values:

$$r_o = 2.8648 \cdot 10^{-10}\,\mathrm{m},$$

$$D/k_B = 30200\,\mathrm{K}, \quad b = 5.81, \quad a = 1.88. \tag{22}$$

The equation of state and various BCC-Nb properties with interatomic potential parameters (22) were calculated in [42,43] by the method from (8)–(15). In [42], the baric dependences of various BCC-Nb properties were calculated along isotherms 300 and 3000 K in the pressure range $P = 0$–200 GPa, and the results show good agreement with the experimental and calculated data obtained by others. These calculations were generalized in [43] for a nanocrystal from a finite number of atoms and variations of baric dependences were studied with reduction of nanocrystal size or shape deformation BCC-Nb. However, dependence $T_m(P)$ for BCC-Nb in [42,43] was calculated using equation (16) at $T_m(0) = 2742$ K. Here, we also calculated dependence $T_m(P)$ using both equations (16) and (17) at $T_m(0) = 2750$ K.

When using potential parameters (22), the following expressions were derived using equations (9)–(15) along

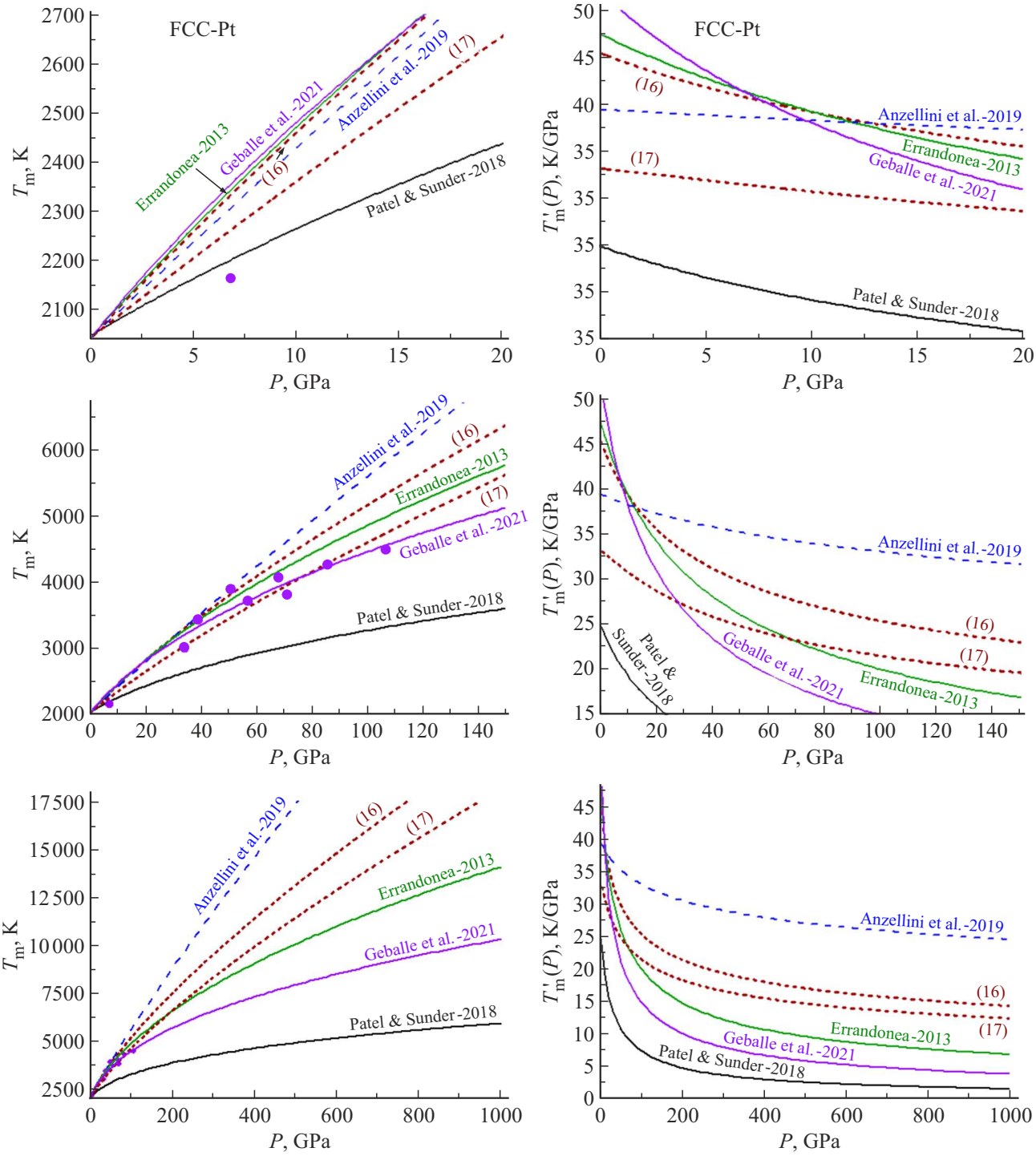

Figure 2. Baric dependences of melting temperature $T_m(P)$ (left graphs) and functions $T'_m(P)$ (right graphs) for FCC-Pt. Solid circles show experimental data for $T_m(P)$ from [38]. Solid lines — dependences (19) and (20) obtained in [35,36,38] on the basis of the experimental data. Dashed lines — calculated dependences (19) and (20) obtained in [37]. Dotted lines — our calculations using equations (16) — upper curve, and (17) — lower curve.

isotherm $T_m(0) = 2750\,\mathrm{K}$ at $P = 0$ for the parameters included in equation (16):

$$c_o(0, T_m(0)) = 2.94338 \cdot 10^{-10}\,\mathrm{m},$$

$$\Theta_o(0, T_m(0)) = 255.4587\,\mathrm{K}.$$

Figure 3 shows baric dependences both for the melting temperature $T_m(P)$ (left graphs) and for the melting temperature derivative with respect to pressure $T'_m(P) = dT_m/dP$ (right graphs) for BCC-Nb. The upper graphs show the low pressure region 0–20 GPa; the lower graphs show

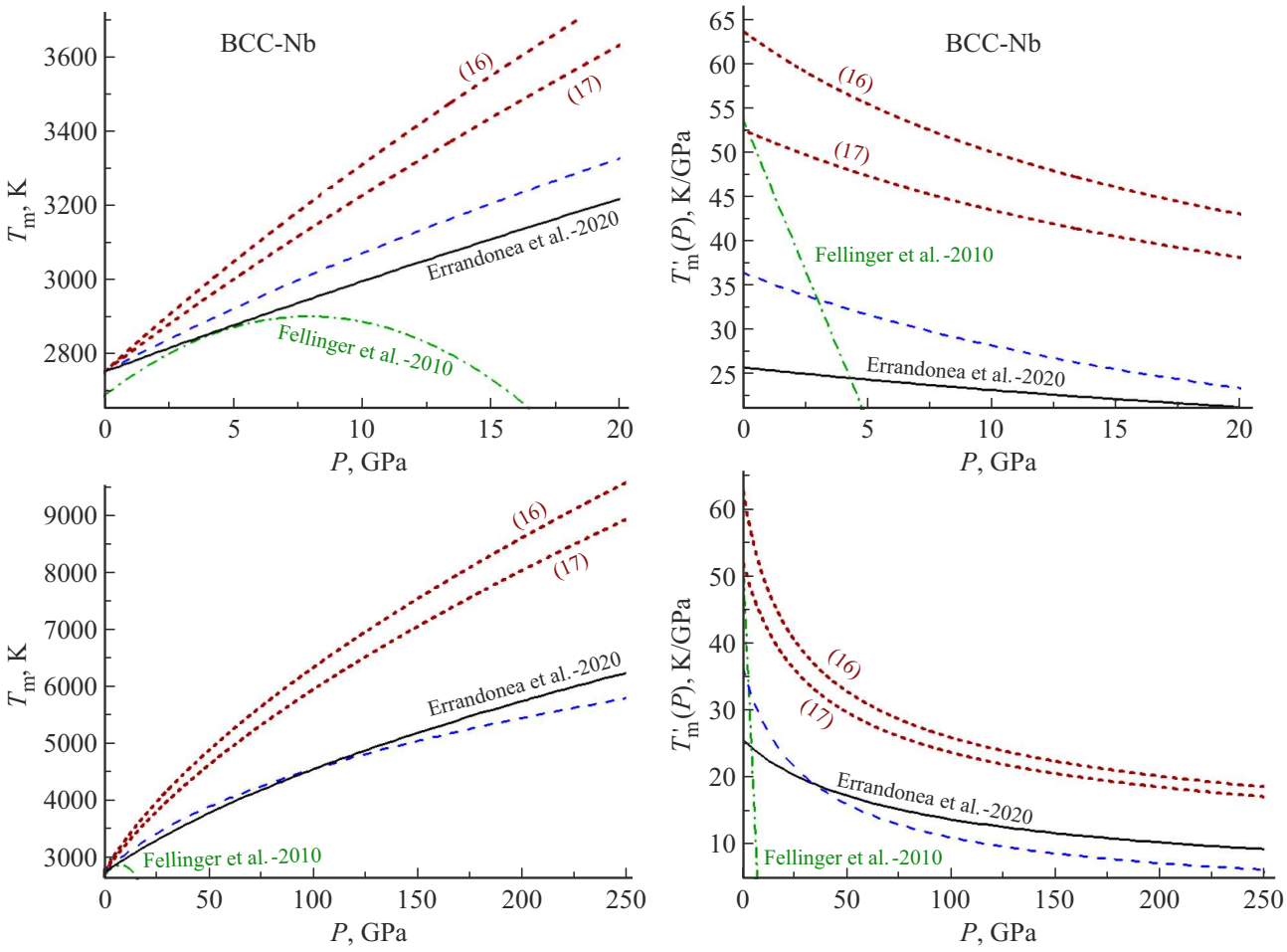

Figure 3. Baric dependences of melting temperature $T_m(P)$ (left graphs) and functions $T'_m(P)$ (right graphs) for BCC-Nb. Solid lines show dependences (19) and (20) experimentally measured in [40]. Dashed lines — theoretical dependences (19) and (20) calculated in [40]. Dash-dot curves show theoretical dependences (23) calculated in [41]. Dotted lines — our calculations using equations (16) — upper curve, and (17) — lower curve.

0−250 GPa pressure region. Dotted lines show dependences $T_m(P)$ and $T'_m(P)$ calculated by us using equations (16) (upper line) and (17) (lower line). Solid line shows the dependence obtained in [40] by fitting seven experimental points measures within 0−120 GPa to the Simon–Glatzel equation (19) with parameters

$$T_{m0} = 2750\,\text{K}, \quad P_0 = 48\,\text{GPa}, \quad c_s = 0.45.$$

The dashed line — is the dependence obtained in [40] by fitting six points calculated in the range from −7.9 to 287 GPa by the quantum molecular dynamics method to the Simon–Glatzel equation (19) with parameters

$$T_{m0} = 2750\,\text{K}, \quad P_0 = 22.6\,\text{GPa}, \quad c_s = 0.30.$$

The dot-dash curve show the dependence obtained in [41] by approximation of 11 points $T_m(P)$ calculated by the molecular dynamics method within 0−2.5 GPa. This

Table 3. Experimental and theoretical (in brackets) values of the melting line inclination at $P = 1$ bar for BCC-Nb

Authors — year	dT_m/dP, K/GPa	Ref.
Errandonea *et al.* — 2020	25.8 (36.5)	[40]
Fellinger *et al.* — 2010	(53.9 ± 0.3)	[41]
Kramynin & Ahmedov — 2019	(62)	[42]
Kramynin — 2022	(65.8)	[43]
Hieu *et al.* — 2022	(22.4)	[44]
This work:		
Eq. (16)	(63.730)	
Eq. (17)	(52.568)	

dependence is written as

$$T_m(P) = T_{m0} + \alpha P + \beta P^2, \quad T'_m(P) = \alpha + 2\beta P, \qquad (23)$$

where $T_0 = 2685.8 \pm 0.2$ K, $\alpha = 53.9 \pm 0.3$ K/GPa, $\beta = -3.4 \pm 0.1$ K/GPa^2.

As shown in Figure 3 and Table 3 for BCC-Nb, our dependence (17) deviates considerably from the experimental dependence from [40] and theoretical dependences obtained by both molecular dynamic method in [40] and analytical statistic method of moments in [44]. However, for calculations in [44], interatomic potential parameters (8) were taken from other studies, where they were defined by other methods. Moreover, [44] did not provided any calculations of the equation of state, i.e. dependences $P(V, T)$, for BCC-Nb within the statistic method of moments used to calculate dependence $T_m(P)$. Thus, the issue of correct pressure calculation is still open.

Deviation of out dependence $T_m(P)$ from the experimental one in [40] may be explained both by the proximity of our calculations for BCC-Nb and other reasons. For example, the following reasons may be provided.

1. This may be attributable to the reduction of the Lindemann parameter from criterion (6) with pressure growth. Similar reduction of the Lindemann parameter with the pressure growth was detected in [10] when melting curves of zirconium (Zr) and hafnium (Hf) were analyzed by the quantum molecular dynamic method.

2. This may be associated with the redistribution of electrons on s−d-orbitals in compression of transition metals with BCC structure. This effect was experimentally found in [45] during investigation of electronic and elastic properties of single-crystal molybdenum (Mo). Variation of electronic density with pressure growth shall result in change of pair interatomic interaction potential parameters (8).

4. Conclusions

A relatively simple analytical (i.e. without computer-based simulation) method for calculation of the melting temperature dependence of a single-component crystal on pressure is offered. The method is based on the Mie−Lennard-Jones paired 4-parameter interatomic interaction potential and delocalization melting criterion and contain no fitting constants.

It is shown that the delocalization criterion of crystal–liquid transition (1) used by us switches to the Lindemann criterion in case of melting, and is reduced to the Löwen criterion in case of crystallization.

The developed method was used to calculate baric dependences of melting temperatures and melting temperature derivative with respect to pressure for gold, platinum and niobium in the pressure range of $P = 0-1000$ GPa. It is shown that the dependences calculated by this method for gold and platinum better agree with the experimental data that the dependences obtained by the computer-based simulation methods.

For niobium, the calculated dependence $T_m(P)$ was steeper, i.e. $T'_m(P)$ was higher than the experimental data obtained in [40]. It is shown that the difference may be attributable to various causes: for example, reduction of the Lindemann parameter with pressure growth [10] or redistribution of electrons on s−d-orbitals in compression of transition metals with BCC structure [45].

Acknowledgments

The author would like to express his gratitude to S.P. Kramynin, N.Sh. Gazanova, Z.M. Surkhayeva and M.M. Gadzhieva for fruitful discussions and assistance in work.

Conflict of interest

The author declares that he has no conflict of interest.

References

[1] N.R. Mitra, D.L. Decker, H.B. Vanfleet. Phys. Rev. **161**, *3*, 613 (1967). https://doi.org/10.1103/PhysRev.161.613
[2] J. Akella, G.C. Kennedy. J. Geophys. Res. **76**, *20*, 4969 (1971). https://doi.org/10.1029/JB076i020p04969
[3] P.W. Mirwald, G.C. Kennedy. J. Geophys. Res.: Solid Earth **84**, *B12*, 6750 (1979). https://doi.org/10.1029/JB084iB12p06750
[4] D. Errandonea. Appl. Phys. **108**, *3*, 033517 (2010). https://aip.scitation.org/doi/abs/10.1063/1.3468149
[5] G. Weck, V. Recoules, J.A. Queyroux, F. Datchi, J. Bouchet, S. Ninet, G. Garbarino, M. Mezouar, P. Loubeyre. Phys. Rev. B **101**, *1*, 014106 (2020). https://doi.org/10.1103/PhysRevB.101.014106
[6] P. Parisiades. Crystals **11**, *4*, 416 (2021). https://doi.org/10.3390/cryst11040416
[7] Q.S. Mei, K. Lu. Progress. Mater. Sci. **52**, *8*, 1175 (2007). https://doi.org/10.1016/j.pmatsci.2007.01.001
[8] J. Ma, W. Li, G. Yang, S. Zheng, Y. He, X. Zhang, X. Zhang, X. Zhang. Phys. Earth. Planetary Interiors **309**, 106602 (2020). https://doi.org/10.1016/j.pepi.2020.106602
[9] D. Ashwini, V.S. Sharma, K. Sunil. Eur. Phys. J. Plus **137**, *545*, 1 (2022). https://doi.org/10.1140/epjp/s13360-022-02733-4
[10] D.V. Minakov, M.A. Paramonov, G.S. Demyanov, V.B. Fokin, P.R. Levashov. Phys. Rev. B **106**, *21*, 214105 (2022). https://doi.org/10.1103/PhysRevB.106.214105
[11] F.A. Lindemann. Physikalische Zeitschrift **11**, *14*, 609 (1910).
[12] J.J. Gilvarry. Phys. Rev. **102**, *2*, 308 (1956). https://doi.org/10.1103/PhysRev.102.308
[13] J.P. Adams, R.M. Stratt. J. Chem. Phys. **93**, *2*, 1332 (1990). https://doi.org/10.1063/1.459145
[14] J.P. Adams, R.M. Stratt. J. Chem. Phys. **93**, *2*, 1358 (1990). https://doi.org/10.1063/1.459146
[15] H. Löwen, T. Palberg, R. Simon. Phys. Rev. Lett. **70**, *10*, 1557 (1993). DOI: https://doi.org/10.1103/PhysRevLett.70.1557
[16] H. Löwen. Phys. Rev. E **53**, *1*, R29 (1996). https://doi.org/10.1103/PhysRevE.53.R29
[17] S.A. Khrapak. Phys. Rev. Res. **2**, *1*, 012040 (2020). https://doi.org/10.1103/PhysRevResearch.2.012040
[18] M.N. Magomedov. Tech. Phys. Lett. **33**, *10*, 837 (2007). https://doi.org/10.1134/S1063785007100094
[19] M.N. Magomedov. Phys. Met. Metallography **105**, *2*, 116 (2008). https://doi.org/10.1134/S0031918X08020038
[20] D.S. Sanditov. JETP **115**, *1*, 112 (2012). https://doi.org/10.1134/S1063776112060143

[21] D.S. Sanditov, B.S. Sydykov. Tech. Phys. **59**, *5*, 682 (2014). https://doi.org/10.1134/S1063784214050272
[22] M.N. Magomedov. Phys. Solid State **64**, *4*, 469 (2022). https://doi.org/10.21883/PSS.2022.04.53504.240
[23] Handbook of Mathematical Functions / Eds M. Abramowitz, I. Stegun. National Bureau of Standards, N.Y. (1964). 1046 p.
[24] A.G. Chirkov, A.G. Ponomarev, V.G. Chudinov. Tech. Phys. **49**, *2*, 203 (2004). https://doi.org/10.1134/1.1648956
[25] G.M. Poletaev, M.D. Starostenkov. Phys. Solid State **51**, *4*, 727 (2009). https://doi.org/10.1134S106378340904012X
[26] M.N. Magomedov. Phys. Solid State **64**, *7*, 765 (2022). https://doi.org/10.21883/PSS.2022.07.54579.319
[27] M.N. Magomedov. Tech. Phys. **58**, *9*, 1297 (2013). https://doi.org/10.1134/S106378421309020X
[28] L.A. Girifalco. Statistical Physics of Materials. J. Wiley & Sons Ltd., N.Y. (1973). 346 p.
[29] R. Briggs, F. Coppari, M.G. Gorman, R.F. Smith, S.J. Tracy, A.L. Coleman, A. Fernandez-Panella, M. Millot, J.H. Eggert, D.E. Fratanduono. Phys. Rev. Lett. **123**, *4*, 045701 (2019). https://doi.org/10.1103/PhysRevLett.123.045701
[30] D.E. Fratanduono, M. Millot, D.G. Braun, S.J. Ali, A. Fernandez-Pañella, C.T. Seagle, J.-P. Davis, J.L. Brown, Y. Akahama, R.G. Kraus, M.C. Marshall, R.F. Smith, E.F. O'Bannon III, J.M. Mcnaney, J.H. Eggert. Science **372**, *6546*, 1063 (2021). https://doi.org/10.1126/science.abh0364
[31] M.N. Magomedov. Phys. Solid State **63**, *9*, 1495 (2021). https://doi.org/10.1134/S1063783421090250
[32] H.K. Hieu, N.N. Ha. AIP Adv. **3**, *11*, 112125 (2013). https://doi.org/10.1063/1.4834437
[33] P.D. Tan, P.D. Tam. Vacuum **198**, 110815 (2022). https://doi.org/10.1016/j.vacuum.2021.110815
[34] N. Van Nghia, N.D. Chinh, H.K. Hieu. Vacuum **202**, 111189 (2022). https://doi.org/10.1016/j.vacuum.2022.111189
[35] D. Errandonea. Phys. Rev. B **87**, *5*, 054108 (2013). https://doi.org/10.1103/PhysRevB.87.054108
[36] N.N. Patel, M. Sunder. AIP Conf. Proc. AIP Publ. LLC **1942**, *1*, 030007 (2018). https://doi.org/10.1063/1.5028588
[37] S. Anzellini, V. Monteseguro, E. Bandiello, A. Dewaele, L. Burakovsky, D. Errandonea. Sci. Rep. **9**, 13034 (2019). https://doi.org/10.1038/s41598-019-49676-y
[38] Z.M. Geballe, N. Holtgrewe, A. Karandikar, E. Greenberg, V.B. Prakapenka, A.F. Goncharov. Phys. Rev. Mater. **5**, *3*, 033803 (2021). https://doi.org/10.1103/PhysRevMaterials.5.033803
[39] J.-M. Joubert, J.-C. Crivello, G. Deffrennes. Calphad **74**, 102304 (2021). https://doi.org/10.1016/j.calphad.2021.102304.hal-03295408
[40] D. Errandonea, L. Burakovsky, D.L. Preston, S.G. MacLeod, D. Santamaría-Perez, S. Chen, H. Cynn, S.I. Simak, M.I. McMahon, J.E. Proctor, M. Mezouar. Commun. Mater. **1**, *1*, 60 (2020). https://doi.org/10.1038/s43246-020-00058-2
[41] M.R. Fellinger, H. Park, J.W. Wilkins. Phys. Rev. B **81**, *14*, 144119 (2010). https://doi.org/10.1103/PhysRevB.81.144119
[42] S.P. Kramynin, E.N. Ahmedov. Phys. Met. Metallography **120**, *11*, 1027 (2019). https://doi.org/10.1134/S0031918X19110097
[43] S.P. Kramynin. Phys. Met. Metallography **123**, *2*, 107 (2022). https://doi.org/10.1134/S0031918X22020065
[44] H.K. Hieu, H. Hoang, P.T.M. Hanh, T.T. Hai. Vacuum **206**, 111507 (2022). https://doi.org/10.1016/j.vacuum.2022.111507
[45] C. Yang, Y. Zhang, N.P. Salke, Y. Bi, A. Alatas, A.H. Said, J. Hong, J.F. Lin. Phys. Rev. B **105**, *9*, 094105 (2022). https://doi.org/10.1103/PhysRevB.105.094105

Translated by E.Ilyinskaya